Can We Fake Gamma Emissions of Nuclear Warheads? An Exploratory Study

Christopher Fichtlscherer, Malte Göttsche and Moritz Kütt

Abstract

Nuclear warhead authentication is a crucial step in nuclear disarmament verification. Obviously, cheating of any kind has to be prevented. While several warhead authentication approaches rely on the passive emissions of a weapon's fissile material, the uniqueness of these signatures has been brought into question repeatedly. It would hamper current verification efforts if malicious actors could replicate or fake these signatures with hoax objects.
In this paper, we evaluate the uniqueness of passive gamma emissions of nuclear weapons. Based on a notional nuclear weapon model available in public literature, we use computer simulations to obtain this model's baseline gamma spectra as they would result from realistic measurements. Then we are looking for combinations of other relevant radioactive isotopes that could generate a similar spectrum and therefore be used to deceive verification measures. The analysis is repeated for multiple measurement technologies. Clearly, the higher the detector resolution is, the harder it is to develop suitable hoax objects. Yet, using lower resolutions has the benefit of providing intrinsic protection of highly sensitive warhead design information. Our results contribute to selecting adequate measurement approaches and discourage cheating more broadly.

Keywords

Gamma Spectroscopy, Imitation of Gamma Emissions, Fetter Model, Gamma Detectors, OpenMC

Introduction

Nuclear warheads emit radioactive signatures. In general, these signatures are considered unique. They could be used to verify compliance with nuclear disarmament agreements or even to ascertain whether the world is free of nuclear weapons. At the same time, states could try to cheat by spoofing the signatures. How difficult would that be? How unique are the radioactive signatures? Although the question of whether warhead signatures are unique has been raised multiple times [DOE 1997], [IPNDV 2017], to our knowledge, no publicly available research exists addressing it. Were the signatures not unique, a state could use hoax objects with radioactive emissions similar to those of nuclear weapons. In this article, we study whether such hoax objects could be produced. The red-team-like approach makes use of extensive computer simulations. To find hoax objects, we start with simple assumptions and continuously increase complexity to end up with an actual notional warhead model. In theory, radioactive objects are always uniquely identifiable by their gamma emissions. But actual measurements of a gamma spectrum, for example, add uncertainties due to finite measurement times and a discretization of a continuous spectrum using a limited number of energy channels. Under such circumstances it seems possible that two different objects' emissions appear as the same measured signal. While that should point us to use always the best available measurement technology, nuclear disarmament verification comes with an added difficulty. Here, a balance has to be found between competing interests. Not only want inspecting parties to gain very high confidence that an object presented is indeed a nuclear weapon, but weapon owners in parallel consider certain information sensitive and require protection of such information. This can be done intrinsically, for example, through limiting a detector resolution. Such limits in turn, increase the possibility for cheating.
States often claim that sharing sensitive information in inspection settings is prohibited by the Nuclear Non-Proliferation Treaty. There, intentional transfer of knowledge relevant to weapons construction and design to non-nuclear weapon states is prohibited. Besides such legal arguments, states also claim national security interests as a reason to keep information secret. They fear that precise knowledge of a weapon design might allow others to find countermeasures against their use. Others argue that the real reason for secrecy is to push nuclear weapons out of the general consciousness and present them as very abstract and complex objects [Samuels 2008].
It is important that the search for an adequate balance in actual warhead authentication processes does not become an impediment to nuclear disarmament efforts. The research presented here should help to determine the least amount of information necessary to avoid manipulation.

Emissions of the Fetter Model

In the late 1980s, intensive cooperation took place between Soviet and American research institutions. U.S. scientists visited a Soviet nuclear test site to install seismic detectors [Broad 1986]. Collaboration continued with a large study on

arms control verification mechanisms [von Hippel and Sagdeev 1990] and culminated in 1989 in the visit of American scientists to measure radiation signatures of a Soviet nuclear weapon as part of the "Black-Sea Experiment" [Fetter, Cochran, et al. 1990; Cochran 2011].
As part of this cooperation, a group of scientists proposed a simple model of a notional implosion-type nuclear weapon. The model is commonly called "Fetter Model", after the first author of the paper in which it was first presented [Fetter, Frolov, et al. 1990]. Figure 1 shows the model consisting of concentric spheres of material. In the following, we will use the photon emissions of this model as a baseline for cheating attempts. Several variants of such a model are given in [Fetter, Frolov, et al. 1990]. We focus in this publication on the plutonium-based model.
Besides gamma spectroscopy, neutron coincidence measurements can also support warhead authentication through passive means but are beyond the scope of this article. Authentication of highly-enriched uranium (HEU) by passive measurements of photons and neutrons is very difficult due to the low activity of the material. For HEU weapons, typically active interrogation methods are discussed.

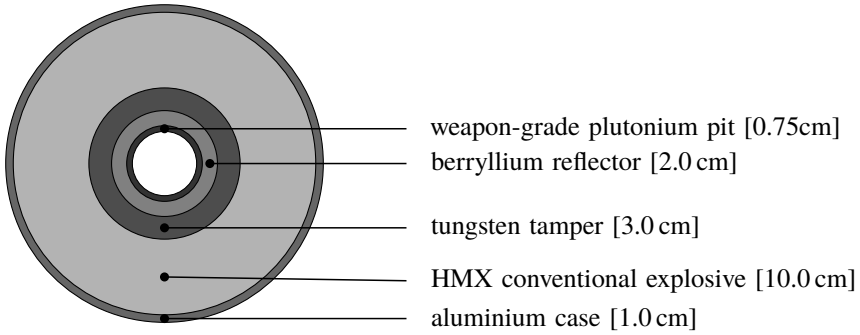

Figure 1. *Notional nuclear weapon model. The values in brackets describe the thickness of each shell. The plutonium shell has an outer radius of 5 cm.*

Isotope	Amount [g]	Number of atoms	Created photons [1/atom/s]	Total created photons [1/s]
O-16	8.0	$3.01 \cdot 10^{23}$	-	-
Pu-238	0.2	$5.06 \cdot 10^{19}$	$1.19 \cdot 10^{-11}$	$6.02 \cdot 10^{9}$
Pu-239	3733.49	$9.41 \cdot 10^{24}$	$8.39 \cdot 10^{-14}$	$7.89 \cdot 10^{11}$
Pu-240	240.1	$6.02 \cdot 10^{23}$	$1.75 \cdot 10^{-13}$	$1.05 \cdot 10^{11}$
Pu-241	17.61	$4.40 \cdot 10^{22}$	$6.24 \cdot 10^{-13}$	$2.75 \cdot 10^{10}$
Pu-242	0.6	$1.49 \cdot 10^{21}$	- [a]	- [a]

Table 1. *Plutonium composition and basic gamma emission intensities.*
[a] *Pu-242 emissions were neglected.*

The composition of the weapon material is given in Table 1. We determined the initial photon emission energies and intensity in plutonium using PyNE 0.7.1 [Scopatz et al. 2012]. The table also shows total intensities per isotope. We then simulated the transport of these gamma particles through the model geometry with the photon functionality [Lund and Romano 2018] of OpenMC. OpenMC is a modern open source Monte Carlo particle transport code [Romano et al. 2015]. The simulations allow us to determine the emissions at the surface of the model. OpenMC uses a simplified physical model and is can simulate the four main interactions of photons: Coherent (Rayleigh) scattering, Compton scattering, photoelectric absorption, and pair production. We used the photon cross section library ENDF-B VII.1. Photon interactions also produce electrons as secondary particles. OpenMC cannot model electron transport but again uses a simplified model to estimate the photons produced by the bremsstrahlung of these electrons. We do not consider photons from neutron interactions with the outer layers of the weapon model [Snowden 2017]. We determined the emissions at the model's surface in a simulation with $2.4 \cdot 10^{10}$ starting particles. Figure 2 shows the energy and intensity of resulting photons in 100 equal energy bins between 0 and 1.0 MeV.

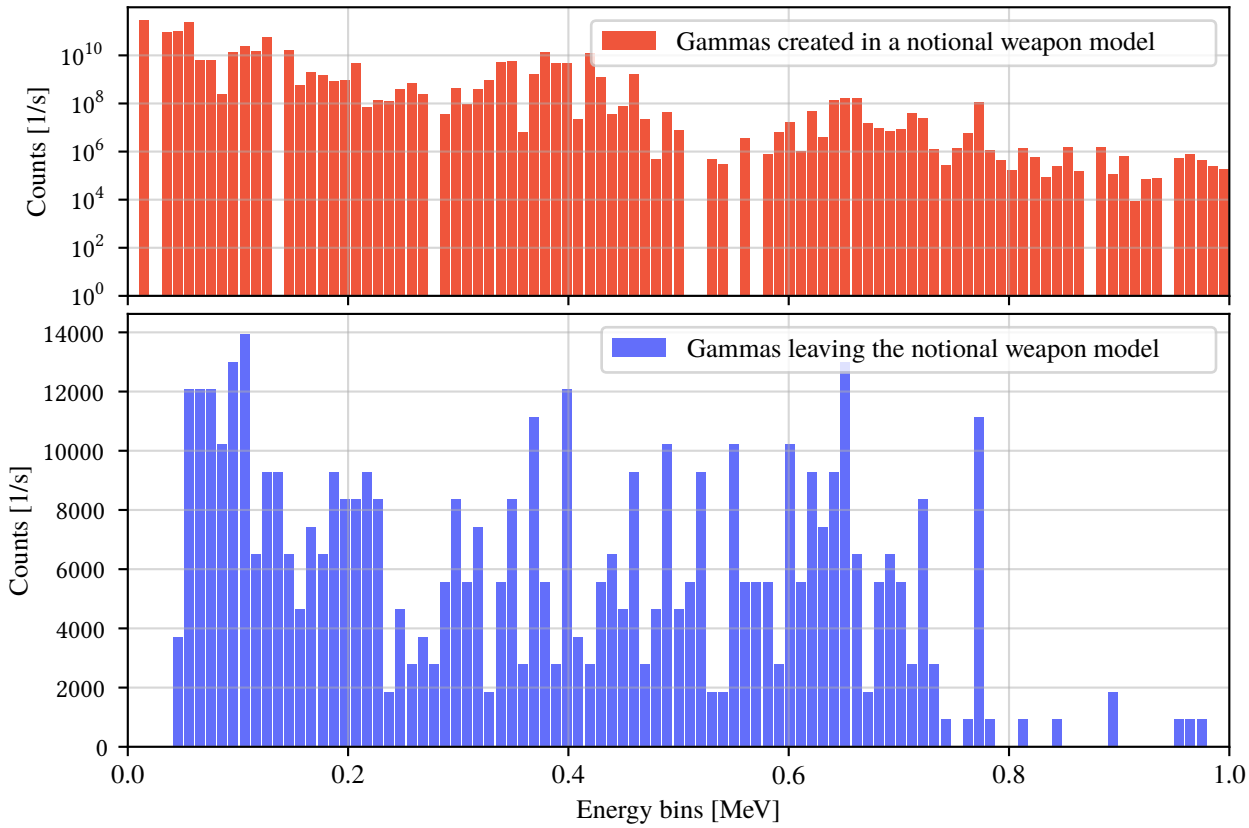

Figure 2. *The created gammas in the Fetter model and the emissions at its surface.*

The emissions include $175.39 \cdot 10^9$ gamma particles with an energy of more than 100 keV per second. Plutonium-239 produces about 77 percent of these gamma particles. One gram plutonium-239 emits on average $2.11 \cdot 10^8$ photons of 167 different energies (in the given range), whereby the peaks with the highest intensity are between 300 and 400 keV. Plutonium-240 and plutonium-241 are responsible for 8 and 14 percent, respectively, plutonium-238 contributes only about 0.04 percent. All these figures are given for a "new" weapon (0 years of age).

Authentication Methods

Several systems have been proposed to authenticate nuclear weapons, developed by either nuclear-weapon states, non-nuclear weapon states, or non-governmental research institutions. Comprehensive overviews of warhead authentication approaches are outlined in [Göttsche and Kirchner 2014] and [Yan and Glaser 2015]. The different measurement devices fall into two broad categories: Devices using an *attribute approach*, in which an object is assumed to be a nuclear weapon if measured properties are within prior defined conditions. These properties could be, for example, the mass of fissile material or a specific geometrical shape. Other devices use a *template approach*, in which an object under inspection is compared to another object. The second object ("template" or "golden sample") is an object of which inspectors believe with high confidence that it is a nuclear weapon. A second distinction can be made between active measurements and passive measurements. While passive measurements measure only the emissions of the nuclear weapon, active measurements record emissions from a weapon that have been induced by prior irradiation with different external sources. Here, we analyze the cheating possibilities for two template approaches using passive low-resolution gamma spectroscopy.

In 2001, Sandia National Laboratories developed the Trusted Radiation Identification System (TRIS) [Seager et al. 2001]. TRIS measures the passive gamma spectrum of an object with 16 energy regions.[1] The system also includes an "Information Barrier" component to show the comparison result without revealing sensitive information of the measured objects. In 2019, the Information Barrier X II (IBX II) was developed at Princeton University [Kütt and Glaser 2019]. It also compares objects by their passive gamma emissions and provides an information barrier. The system uses vintage electronics to reduce vulnerabilities of malicious hardware manipulations. Table 2 shows the used

1. One of these bins consists of the counts from two different energy regions.

energy regions for both systems.

Authentication System	Detector	Energy bins [keV]
TRIS	NaI scintillation crystal 2” dia. x 2” thick	[80 - 120], [120 - 160], [160 - 172], [172 - 198], [198 - 230], [230 - 290],[290 - 350] & [390 - 500], [350 - 390], [500 - 600], [600 - 711], [711 - 821], [821 - 936], [936 - 1090], [1090 - 1200], [1200 - 2480], [2480 - 2750]
IBX II	Mirion 802 Scintillation Detector [Mirion Technology Inc 2017] 2” dia. x 2” thick	[0 - 197], [197 - 451], [451 - 706], [706 - 960], [960 - 1215], [1215 - 1469], [1469 - 1724], [1724 - 1978], [1978 - 2233], [2233 - 2487], [2487 - 2742], [2742 - 2950]

Table 2. *Two gamma spectroscopy based warhead authentication systems. The systems record gamma spectra within the energy bins given in the table.*

Both systems use a sodium-iodide scintillation detector. The procedure of comparisons between the template and the measurement result afterward is very similar. The IBX II uses a simplified chi-squared test

$$\chi^2 = \sum_{i=1}^{12} \frac{(M_i - T_i)^2}{T_i}, \tag{1}$$

in which T_i is the number of counts of energy bin i of the template, and M_i is the respective number of counts of the current measurement. The data is not normalized to the measurement time. In our theoretical simulations below, some template channels will have zero counts. For the calculations of chi-squared presented here, we omit these values. In practical applications, it is highly unlikely that energy bins remain completely without counts. If $\chi^2 < 100$, IBX II assumes that the two spectra are identical within statistical errors [Kütt and Glaser 2019]. It should be noted that the chi-squared test scales linearly with measurement time. Thus, by doubling the measurement time, the chi-squared value increases by a factor of two.

TRIS uses the reduced chi-squared test, where the test result is divided by the degrees of freedom f of the system. Here, we assume the degrees of freedom as the number of the non-zero energy bins of the template.

$$\chi_r^2 = \frac{1}{f} \cdot \sum_{i=1}^{16} \frac{(M_i - T_i)^2}{T_i}. \tag{2}$$

TRIS will accept the object if $\chi_r^2 < 4$ [Seager et al. 2001]. For this paper, we assumed that all energy bins are equally weighted. Future research could analyze weight factors such that cheating attempts are complicated. Through such an approach, certain isotopes currently attractive for hoax objects could be specifically excluded.

Simulation of the Detector Response

For both systems, we modeled a simplified version of the scintillation detector in OpenMC. Through extensive simulations, we generated a general-purpose detector response function. The simulations rely on a newly developed pulse-height tally functionality in OpenMC [Fichtlscherer et al. 2021]. Gaussian energy broadening was applied to the resulting spectra to account for the limited detector resolution. The response function was generated from 300 separate simulations for incoming gamma particles with energies of 10 keV, 20 keV, ..., 3 MeV. Every simulation used 10^7 particles and the photon interaction cross section library ENDF/B-VII.1. Figure 3 shows the resulting spectra, including characteristic peaks.

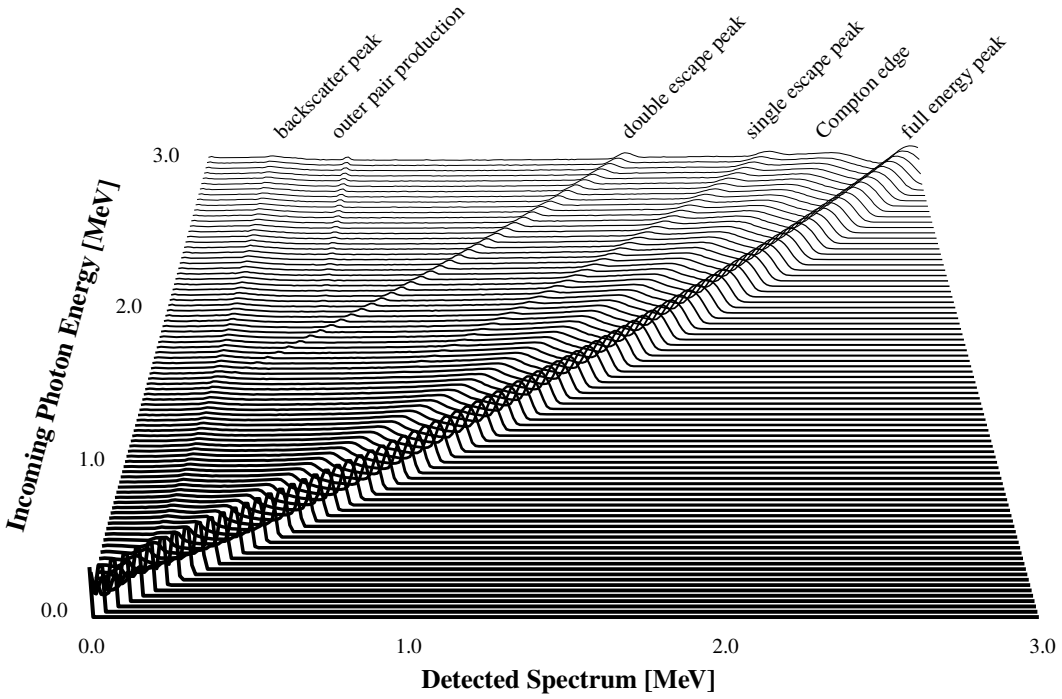

Figure 3. *Detector response matrix of a 2 by 2 inch sodium-iodide scintillation detector. Individual spectra were simulated using a pulse-height tally function and include Gaussian energy broadening to account for the detector resolution.*

To determine initial gamma energy levels and intensities for radioactive isotopes, we use data provided by PyNE 0.7.1 [Scopatz et al. 2012]. To estimate the detector response for gamma energies between the simulated energies, linear interpolation was used. For example, we determine the detector response for cesium-137 (661.7 keV photon emission) by using 0.83 times the 660 keV spectrum plus 0.17 times the 670 keV spectrum. For the total detector response of an isotope, we use the intensity-weighted sum of the different emission lines. To simplify the analysis of the measurements using TRIS and IBX II, we used the respective energy bins. To construct the hoax object, we consider a total number of 223 non-stable isotopes with a half-life of one week or longer. For obvious reasons, we exclude Pu-239. Other isotopes of plutonium are included to check whether states could construct hoax objects, including plutonium.[2]

Searching for Potential Hoax Objects

We searched for theoretical hoax objects that produce the same detector signal in IBX II or TRIS for different measurements: A plutonium-239 point source of mass 1 g and the notional nuclear weapon model described above. The hoax objects are assumed as point sources. For this theoretical study, we neglect several limiting factors in the real world: We do not investigate the difficulties to obtain certain isotopes, the precision chemistry required to create the proposed material mixtures, nor the chemical stability of the mixtures. We also do not consider any shielding and neglect self-shielding effects. Given the small amounts of material required, self-shielding is likely not an issue anyway. The other limitations could apply. However, it is also reasonable to assume that a state with the capability to build nuclear weapons and later the intention to cheat in the disarmament process would go to great lengths and invest significant resources in producing hoax objects.

The hoax objects are found through simple mathematical optimization. We search for that linear combination (with positive coefficients) of the isotopes' detector responses that most closely match the simulated measurement signal. This means solving the Non-Negative Least Squares (NNLS) problem

$$\arg\min_h \|Rh - t\|_2^2 \quad \text{subject to} \quad h \geq 0. \tag{3}$$

Here, h is a vector containing the number of atoms for each of the 223 radioactive isotopes considered. The matrix R contains their detector response functions, t is the template signal. We performed this optimization step with the NNLS

2. Furthermore, we currently omit Ag-105, Ac-227, Th-229, Pa-223, and Cf-252, because PyNE 0.7.1 does not provide information about their gamma emissions.

algorithm [Lawson and Hanson 1995], which is part of the Pythons SciPy package [Virtanen et al. 2020].
After determining the isotope combination of the hoax object, we calculate the chi-squared test result between the emissions of the hoax object and the template. For these results, we assume a measurement time of one second and detection efficiency of 1. The chi-squared scales linear with the total count rate. To calculate values for real measurements, the values presented here must be multiplied by the measurement time and the absolute detector efficiency.

While we search for hoax objects minimizing the mean least-square error of the emissions in a very general approach, for IBX II and TRIS, we could also directly minimize the chi-squared value. This would add complexity but might allow us to find even "better" hoax objects for these particular systems. Also, one could modify the search process to place the error in particular bins; for example, one could exploit the statistical error bounds that are specified for the different TRIS bins.

To look for further hoax objects, we carried out more optimization steps, excluding those isotopes suitable as hoax objects in previous steps. Through this procedure, we can show the variety of possible isotope combinations. Whenever we find at least two suitable hoax objects, we can, in fact, create an infinite number of new isotope combinations from linear combinations of those.

Results

Figures 4 and 5 summarize the results for potential hoax objects for plutonium-239 and the notional weapon model. The tables list different isotope combinations that are similarly usable. It is noticeable that the isotopes have very high activity. Therefore, significantly less material is required for hoax objects. While for example, 1 g of plutonium-239 emits $2.11 \cdot 10^8$ photons every second, only 0.42 ng of selenium-72 emits $1.91 \cdot 10^8$ photons per second. The bar charts show the results for individual bins for hoax object 1 in each case. For all four combinations of detection systems and measurement scenarios, we find combinations of isotopes very suitable to fool the authentication procedures.
The tables also include the calculation of chi-squared tests as used in IBX II and TRIS. All results assume that the detector registers the total number of source photons.
Only the hoax object found for TRIS measuring a notional weapon signature exhibits a small number in upper bin regions (1090-1200 keV: 16.2 counts per second, 1200-2480 keV: 5.7 counts per second). As we consider the original object as the "template", these two bins are not included in our chi-squared calculation. In real applications, all bins would have some background counts; hence they would also be taken into account. However, given that the count rate in these bins is three orders of magnitude smaller than the next larger one, the effects still should be negligible.

Hoax object 1 (IBX II) ($\chi^2 = 4.17 \cdot 10^{-23}$)	Hoax object 2 (IBX II) ($\chi^2 = 2.88 \cdot 10^{-23}$)	Hoax object 3 (IBX II) ($\chi^2 = 2.79 \cdot 10^{-19}$)	Hoax object 1 (TRIS) ($\chi_r^2 = 1.18 \cdot 10^{-23}$)	Hoax object 2 (TRIS) ($\chi_r^2 = 2.80 \cdot 10^{-20}$)
Se-72 (0.42 ng)	**Rb-86** ($1.98 \cdot 10^{-5}$ ng)	**Sc-46** ($4.04 \cdot 10^{-11}$ ng)	**Cr-51** ($3.23 \cdot 10^{-3}$ ng)	**Be-7** ($3.95 \cdot 10^{-2}$ ng)
Nb-95 ($3.35 \cdot 10^{-4}$ ng)	**Zr-95** ($6.16 \cdot 10^{-4}$ ng)	**Mn-54** ($1.09 \cdot 10^{-3}$ ng)	**Mn-54** ($3.51 \cdot 10^{-5}$ ng)	**Co-57** (0.47 ng)
Te-121 ($2.85 \cdot 10^{-3}$ ng)	**Ru-103** ($5.43 \cdot 10^{-3}$ ng)	**Co-58** ($1.65 \cdot 10^{-15}$ ng)	**Zn-65** ($1.15 \cdot 10^{-12}$ ng)	**Zr-95** ($4.26 \cdot 10^{-4}$ ng)
Lu-171 ($4.61 \cdot 10^{-18}$ ng)	**Sn-117*** (0.75 ng)	**Zn-65** ($3.38 \cdot 10^{-5}$ ng)	**Rb-86** ($5.42 \cdot 10^{-7}$ ng)	**Rh-101** (0.61 ng)
Hf-178* ($9.56 \cdot 10^{-8}$ ng)	**Hf-179*** ($1.17 \cdot 10^{-6}$ ng)	**I-131** ($2.29 \cdot 10^{-3}$ ng)	**Nb-95** ($3.07 \cdot 10^{-4}$ ng)	**Pd-103** (35.7 ng)
Pa-230 ($1.63 \cdot 10^{-5}$ ng)	-	**Gd-146** (2.10 ng)	**Gd-146** ($8.74 \cdot 10^{-3}$ ng)	**Sn-113** ($6.91 \cdot 10^{-2}$ ng)
-	-	**Tm-167** ($9.76 \cdot 10^{-2}$ ng)	**Tm-167** ($2.56 \cdot 10^{-3}$ ng)	**Sb-125** ($8.63 \cdot 10^{-2}$ ng)
-	-	-	**Hf-175** (0.11 ng)	**Ba-140** ($4.54 \cdot 10^{-2}$ ng)
-	-	-	**Hf-178*** ($5.70 \cdot 10^{-9}$ ng)	**Ce-141** ($1.29 \cdot 10^{-2}$ ng)
-	-	-	**Hf-181** ($6.80 \cdot 10^{-2}$ ng)	**Nd-147** ($3.01 \cdot 10^{-3}$ ng)
-	-	-	**Pt-188** ($1.61 \cdot 10^{-2}$ ng)	**Gd-153** (0.91 ng)
-	-	-	**Os-191** (0.34 ng)	**Os-185** ($2.02 \cdot 10^{-4}$ ng)
-	-	-	**Tl-202** ($4.69 \cdot 10^{-3}$ ng)	**Pa-230** ($1.31 \cdot 10^{-5}$ ng)
-	-	-	**Th-234** (0.98 ng)	**Es-252** ($1.41 \cdot 10^{-3}$ ng)
-	-	-	**Cm-241** ($9.51 \cdot 10^{-2}$ ng)	-

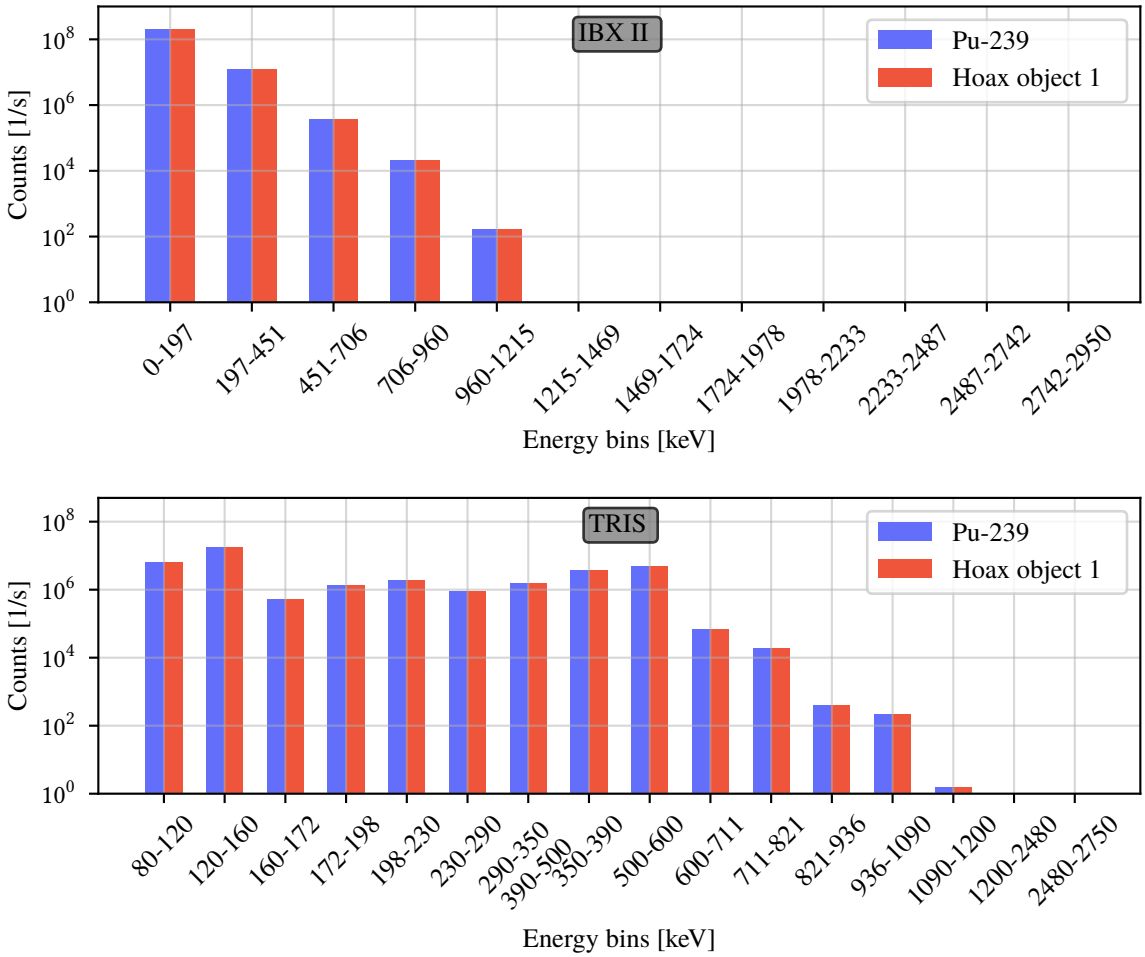

Figure 4. *Potential hoax object composition to imitate the signature of 1 g plutonium-239 (top). Measurement results for hoax object 1 in comparison with real source using IBX II (center) and TRIS (bottom).*

Hoax object 1 (IBX II) ($\chi^2 = 9.99 \cdot 10^{-26}$)	Hoax object 2 (IBX II) ($\chi^2 = 6.95 \cdot 10^{-25}$)	Hoax object 3 (IBX II) ($\chi^2 = 5.33 \cdot 10^{-25}$)	Hoax object 1 (TRIS) ($\chi^2_r = 4.45 \cdot 10^{-7}$)	Hoax object 2 (TRIS) ($\chi^2_r = 9.22 \cdot 10^{-4}$)
Se-72 ($8.86 \cdot 10^{-5}$ ng)	**Co-58** ($1.13 \cdot 10^{-17}$ ng)	**Mn-54** ($2.62 \cdot 10^{-3}$ ng)	**Sr-89** (0.19 ng)	**Cr-51** ($3.15 \cdot 10^{-3}$ ng)
Nb-95 ($4.8886 \cdot 10^{-4}$ ng)	**Rb-86** ($1.09 \cdot 10^{-4}$ ng)	**Fe-59** ($7.31 \cdot 10^{-20}$ ng)	**Nb-92*** ($2.42 \cdot 10^{-6}$ ng)	**Rh-101** ($3.46 \cdot 10^{-3}$ ng)
Te-121 ($1.3586 \cdot 10^{-3}$ ng)	**Nb-92*** ($1.29 \cdot 10^{-19}$ ng)	**Zn-65** ($1.87 \cdot 10^{-4}$ ng)	**Zr-95** ($4.79 \cdot 10^{-4}$ ng)	**Ag-108*** (1.52 ng)
Hf-178* ($3.9186 \cdot 10^{-10}$ ng)	**Zr-95** ($9.20 \cdot 10^{-4}$ ng)	**Tc-95*** ($1.13 \cdot 10^{-16}$ ng)	**Nb-95** ($2.93 \cdot 10^{-5}$ ng)	**Xe-131*** ($6.15 \cdot 10^{-4}$ ng)
Pa-230 ($8.9886 \cdot 10^{-5}$ ng)	**Ru-103** ($2.27 \cdot 10^{-3}$ ng)	**Rh-102** ($9.56 \cdot 10^{-19}$ ng)	**Xe-129*** ($1.61 \cdot 10^{-4}$ ng)	**Pr-143** (2.37 μg)
-	**Sn-117*** ($2.29 \cdot 10^{-4}$ ng)	**Ag-106*** ($3.91 \cdot 10^{-23}$ ng)	**Cs-137** (0.56 ng)	**Pm-144** ($4.35 \cdot 10^{-3}$ ng)
-	**Cs-136** ($6.90 \cdot 10^{-20}$ ng)	**Sn-125** ($5.70 \cdot 10^{-21}$ ng)	**Ce-139** ($1.90 \cdot 10^{-4}$ ng)	**Tb-158** (0.25 ng)
-	**Hf-179*** ($6.40 \cdot 10^{-9}$ ng)	**I-131** ($1.31 \cdot 10^{-4}$ ng)	**Tm-170** ($5.36 \cdot 10^{-2}$ ng)	**Yb-169** ($1.88 \cdot 10^{-4}$ ng)
-	-	**Cm-241** ($5.21 \cdot 10^{-3}$ ng)	**Hf-179*** ($8.20 \cdot 10^{-10}$ ng)	**Os-185** ($1.94 \cdot 10^{-3}$ ng)
-	-	**Pu-246** ($4.53 \cdot 10^{-4}$ ng)	**Tl-202** ($2.55 \cdot 10^{-4}$ ng)	**W-188** ($1.25 \cdot 10^{-3}$ ng)
-	-	-	**Ra-226** (0.12 μg)	**Po-206** ($7.62 \cdot 10^{-6}$ ng)
-	-	-	**Pa-230** ($1.37 \cdot 10^{-4}$ ng)	**Cm-245** (51.3 ng)
-	-	-	**Bk-249** (96.4 μg)	**Es-254** (0.49 ng)
-	-	-	**Es-252** ($2.60 \cdot 10^{-2}$ ng)	-

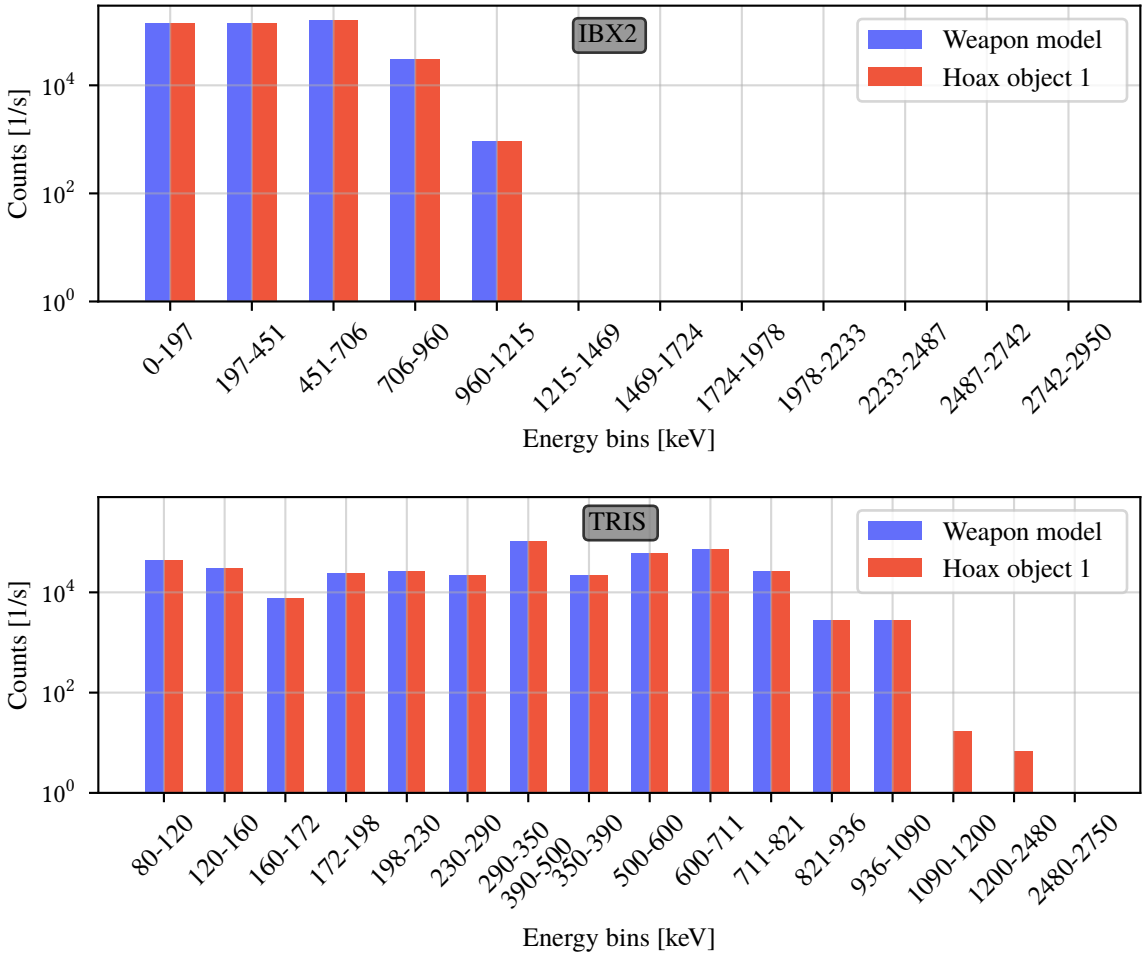

Figure 5. *Potential hoax object composition to imitate the signature of a warhead model (top). Measurement results for hoax object 1 in comparison with real source using IBX II (center) and TRIS (bottom).*

How to Prevent Cheating?

The previous section demonstrated that for the existing systems, cheating is, in principle, possible. An easy way to mitigate the risk of cheating is an increase in measurement resolution – a higher number of energy bins. Here, we used the energy range of IBX II, 0 MeV to 3 MeV. We then analyzed the signal of a notional weapon model and searched for the best possible hoax object for an increasing number of equally-spaced energy bins. For each number of energy bins, we produced hoax objects separately. From these results, we calculated the chi-squared test between the weapon model and the signal of the hoax objects. Figure 6 summarizes the results for up to 50 energy bins. For a single measurement, IBX II records $2^{18} = 262,144$ events. In the figure, the chi-squared test results are calculated based on the same total number of events. IBX II rejects an object if the result of the chi-squared test is greater than 100. With at least 41 energy bins, the hoax object could be distinguished from a real object. For a few subsequent bin numbers, the system could be cheated again. At higher bin numbers, the reliability increases, and the system can always detect a hoax object. In the future, we will also study non-equal width energy bins, similar to those used by TRIS.

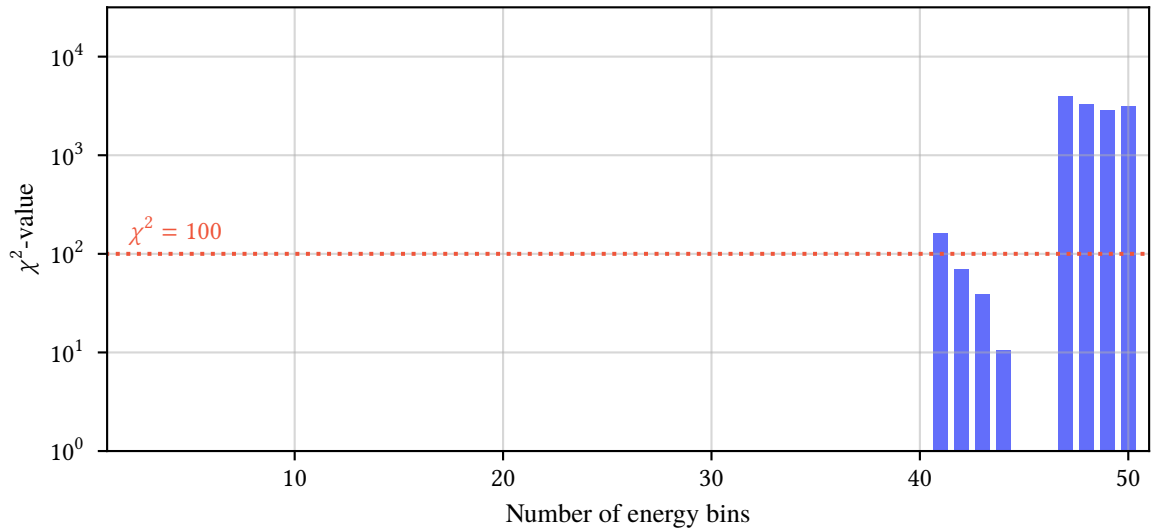

Figure 6. *Number of equally-spaced energy bins between 0 MeV and 3 MeV and the associated chi-squared distance between the best hoax object and the emissions of a notional nuclear weapon model.*

Conclusion and Outlook

Within this article, we presented a first analysis of the uniqueness of nuclear weapons' radiation signatures. Such an analysis is important for future efforts in nuclear disarmament verification, as it determines the potential of cheating. We showed theoretical vulnerabilities for the measurement approaches used by the proposed warhead authentication systems TRIS and IBX II. Within our assumptions, we find that it is possible to replicate certain nuclear weapon signatures using mixtures of other isotopes. Used in a disarmament setting, states could pretend to disarm nuclear weapons while presenting custom-made hoax objects to inspectors. We did not extend our investigation to include signatures beyond gamma radiation. It is relatively easy to detect the absence of neutron emissions from an object, which would reveal our proposed manipulations. Also, it might be relatively difficult to manufacture the hoax objects presented here. Still, the results clearly point to the necessity of additional and more intensive studies, in particular, because it is not unlikely that similar deception possibilities exist for other passive gamma emission-based systems.

Future research could address several issues. First, our analysis could be expanded to more realistic scenarios, including more complex weapon designs, transport containers, and the measurement environment. Second, other signatures should be studied as well. Future studies could focus, for example, on neutron emissions. With methods similar to those presented here one could explore whether neutron signatures could be replicated by other means. Third, finding remedies for the shown vulnerabilities. We present a first and simple solution at the end of the article. By increasing the overall measurement resolution, here through additional energy bins, we showed threshold levels for which hoax object design becomes difficult to impossible. Such an analysis could be expanded to find the "sweet-spot" of verification measurements, which is just fine-grained enough to prevent cheating, but at the same time coarse enough to limit the release of sensitive information. We will take on several of these questions in the near future. Finding adequate answers could help us better understand verification approaches and increase the trust among those using them to achieve future reductions of nuclear weapons.

References

Broad, William J. 1986. Westerners Reach Soviet to Check Atom Site. *The New York Times: U.S.,* July 6, 1986. Available at <https://www.nytimes.com/1986/07/06/us/westerners-reach-soviet-to-check-atom-site.html>.

Cochran, Thomas B. 2011. Black Sea Experiment. Natural Resources Defense Council. Available at <https://www.nrdc.org/sites/default/files/nuc_11020401a.pdf>.

Fetter, Steve, Thomas B. Cochran, Lee Grodzins, Harvey L. Lynch, and Martin S. Zucker. 1990. Gamma-Ray Measurements of a Soviet Cruise-Missile Warhead. *Sciences* 248 (4957): 828–834. Available at <https://science.sciencemag.org/content/248/4957/828>.

Fetter, Steve, Valery A. Frolov, Marvin Miller, Robert Mozley, Oleg F. Prilutsky, Stanislav N. Rodionov, and Roald Z. Sagdeev. 1990. Detecting Nuclear Warheads. *Sciences & Global Secuity* 1 (3-4): 225–253. https://doi.org/10.1080/08929889008426333.

Fichtlscherer, Christopher, Friederike Frieß, Malte Göttsche, and Moritz Kütt. 2021. Implementation and Validation of the Pulse-Height Tally in OpenMC. In INMM & ESARDA Joint Virtual Annual Meeting 2021.

Göttsche, Malte, and Gerald Kirchner. 2014. Measurement techniques for warhead authentication with attributes: Advantages and limitations. *Science & Global Security* 22 (2): 83–110. https://doi.org/10.1080/08929882.2014.918805.

International Partnership for Nuclear Disarmament Verification. 2017. Phase I Summary Report: Creating the Verification Building Blocks for Future Nuclear Disarmament, Available at <https://www.nti.org/analysis/reports/ipndv-phase-i-summary-report-creating-verification-building-blocks-future-nuclear-disarmament/>.

Kütt, Moritz, and Alexander Glaser. 2019. Vintage electronics for trusted radiation measurements and verified dismantlement of nuclear weapons. *PLoS ONE* 14 (10): e0224149. https://doi.org/10.1371/journal.pone.0224149.

Lawson, Charles L, and Richard J Hanson. 1995. *Solving least squares problems.* SIAM. https://doi.org/10.1137/1.9781611971217.

Lund, Amanda L., and Paul K. Romano. 2018. Implementation and Validation of Photon Transport in OpenMC. ANL/MCS-TM-381. Argonne National Laboratory. https://doi.org/10.2172/1490825. Available at <https://www.osti.gov/biblio/1490825-implementation-validation-photon-transport-openmc>.

Mirion Technology Inc. 2017. 802 Scintillation Detectors. Accessed: 2021-07-24, https://www.mirion.com/products/802-scintillation-detectors.

Romano, Paul K., Nicholas E. Horelik, Bryan R. Herman, Adam G. Nelson, Benoit Forget, and Kord Smith. 2015. OpenMC: A state-of-the-art Monte Carlo code for research and development. *Annals of Nuclear Energy* 82:90–97. https://doi.org/10.1016/j.anucene.2014.07.048.

Samuels, David. 2008. Atomic John - A truck driver uncovers secrets about the first nuclear bombs. *The New Yorker* (December 7, 2008). Available at <https://www.newyorker.com/magazine/2008/12/15/atomic-john>.

Scopatz, Anthony, Paul K. Romano, Paul P.H. Wilson, and Katy D. Huff. 2012. PyNE: Python for Nuclear Engineering. In Am. Nuc. Soc. Winter Meeting 2012, vol. 107. San Diego, CA, USA.

Seager, Kevin D, Dean J Mitchell, Thomas W Laub, Keith M Tolk, Richard L Lucero, and Kenneth W Insch. 2001. Trusted Radiation Identification System. In 43rd Annual Meeting of the Institute of Nuclear Materials Management (INMM), Indian Wells, CA.

Snowden, Mareena Robinson. 2017. Nuclear warhead monitoring: a study of photon emissions from fission neutron interactions with high explosives as a tool in arms control verification. PhD diss., Massachusetts Institute of Technology.

United States Department of Energy, Office of Arms Control and Nonproliferation. 1997. Transparency and Verification Options: An Initial Analysis of Approaches for Monitoring Warhead Dismantlement. *Nuclear Instruments and Methods in Physics Research Section B: Beam Interactions with Materials and Atoms,* Available at <https://fas.org/sgp/othergov/doe/dis/transparency.pdf>.

Virtanen, Pauli, Ralf Gommers, Travis E. Oliphant, Matt Haberland, Tyler Reddy, David Cournapeau, Evgeni Burovski, et al. 2020. SciPy 1.0: Fundamental Algorithms for Scientific Computing in Python. *Nature Methods* 17:261–272. https://doi.org/https://doi.org/10.1038/s41592-019-0686-2.

Von Hippel, Frank, and Roald Z. Sagdeev, eds. 1990. *Reversing the Arms Race: How to Achive and Verify Deep Reductions in the Nuclear Arsenals;* Science & Global Security / Monograph Series 1. Gordon and Breach Science Publ.

Yan, Jie, and Alexander Glaser. 2015. Nuclear warhead verification: A review of attribute and template systems. *Science & Global Security* 23 (3): 157–170. https://doi.org/10.1080/08929882.2015.1087221.

Authors

Christopher Fichtlscherer
Institute for Peace Research and Security Policy at the University of Hamburg, Hamburg, Germany - fichtlscherer@ifsh.de
RWTH Aachen University, Aachen, Germany
Malte Göttsche
RWTH Aachen University, Aachen, Germany
Moritz Kütt
Institute for Peace Research and Security Policy at the University of Hamburg, Hamburg, Germany

Acknowledgements

This work was supported by the German Foundation for Peace Research (DSF) through the research project “Nuclear Warhead Authentication Based on Gamma and Neutron Emissions - How to Discourage Cheating?” Malte Göttsche’s contribution is supported by the Volkswagen Foundation. The authors also would like to thank Jan Elfes for his help with the initial development of an OpenMC model of the notional nuclear warhead by Fetter et al.. Parts of the computer simulations carried out for this paper were performed using computing resources granted by RWTH Aachen University under project rwth0572.